LEO Download Capacity Analysis for a Network of Adaptive Array Ground Stations

Mary Ann Ingram[†], William C. Barott[†], Zoya Popovic[¥], Sébastien Rondineau[¥], John Langley[§], Robert Romanofsky*, Richard Q. Lee*, Félix Miranda*, Paul Steffes[†], and Dan Mandl[‡]

[†]Georgia Institute of Technology, Atlanta, GA 30332-0250,
*NASA GRC,21000 Brookpark Rd, Cleveland OH 44135, [¥]University of Colorado, Boulder, CO 80309-0425, [§]Saquish Group, POB 3554, Half Moon Bay, CA 94019, [‡]NASA GSFC, Code 584, Greenbelt, MD 20771

***Abstract* – To lower costs and reduce latency, a network of adaptive array ground stations, distributed across the United States, is considered for the downlink of a polar-orbiting low earth orbiting (LEO) satellite. Assuming the X-band 105 Mbps transmitter of NASA's Earth Observing 1 (EO-1) satellite with a simple line-of-sight propagation model, the average daily download capacity in bits for a network of adaptive array ground stations is compared to that of a single 11 m dish in Poker Flats, Alaska. Each adaptive array ground station is assumed to have multiple steerable antennas, either mechanically steered dishes or phased arrays that are mechanically steered in azimuth and electronically steered in elevation. Phased array technologies that are being developed for this application are the space-fed lens (SFL) and the reflectarray. Optimization of the different boresight directions of the phased arrays within a ground station is shown to significantly increase capacity; for example, this optimization quadruples the capacity for a ground station with eight SFLs. Several networks comprising only two to three ground stations are shown to meet or exceed the capacity of the big dish. Cutting the data rate by half, which saves modem costs and increases the coverage area of each ground station, is shown to increase the average daily capacity of the network for some configurations.**

I. INTRODUCTION[1]

A typical ground station for NASA's low-earth orbiting (LEO) satellites utilizes a single large (10 m – 11 m) dish antenna, and tracks a single satellite at a time by mechanically scanning the antenna through as much as 160 degrees. The downlink supports data rates ranging from 2 kbps up to 150 Mbps. To maximize contact with these polar-orbiting but precessing satellites, the ground stations are near the poles. The ground stations cost from $2M to $4M each to build and have an associated maintenance cost.

It will be shown that it is possible to construct a network with lower-cost ground stations, not necessarily located near the poles, which will receive data from these satellites by adaptively combining several small antennas. When used with current satellites, these networks can provide average daily data rates that meet or exceed the current rates of the large antenna ground stations and use as few as 3 or 4 antennas per ground station, such that each antenna has an aperture size of 0.75m. Variable bit rate methods can further reduce the number of antennas for the entire network. Furthermore, although the subarctic locations of current ground stations maximize the amount of data that can be received per day, it might be cost effective to place the phased arrays at more accessible locations, such as on top of buildings in urban areas. Also, since a distributed network increases the amount of time that a satellite can transmit data, the bandwidth of the satellites can be reduced without compromising the average daily data rates.

Our vision is that the ground stations would be connected via the Internet, so that any given LEO satellite can be in nearly continuous communication with the network on Earth. While the focus of the current project is for a ground station to communicate with only one satellite at a time, the architecture being studied is capable of a rapidly and electronically controlled reconfiguration, to enable fast switching from one satellite to another within the same constellation, or simultaneous communication with multiple satellites.

Two phased array technologies are being investigated for use as the "small antennas" in the proposed ground station. One, which is being developed at the University of Colorado, is the space-fed lens (SFL) array. The SFL is composed of a feed array and a radiating array with each corresponding element pair interconnected by transmission lines of different lengths to radiate a plane wave in the forward direction. The other, being developed at NASA's Glenn Research Center, is the reflectarray (RA). The RA has a surface containing integrated phase shifters and patch radiators; the surface is illuminated by a single feed at a virtual focus. The signal passes through the reflect-mode phase shifters and is re-radiated as a collimated beam in essentially any preferred direction in the field of view of the antenna. Both approaches provide electronic beam steering in elevation, mechanical steering in azimuth, and promise low cost.

It will be shown that the cost of the network is greatly reduced if optimizations are performed for a variable bit rate (VBR) link or array pattern synthesis. Because the ground station requirements in a LEO communications system are determined by the maximum distance between the satellite and the ground station, the system exhibits an excess signal power of up to 12dB when the satellite is close to the ground station. VBR and pattern synthesis methods increase the effi-

This work was supported by the National Aeronautics and Space Administration, Earth-Sun System Technology Office (ESTO), under Grant Number NAG5-13362.

ciency of the ground station by ensuring that the received signal power remains near the desired value regardless of the distance between the satellite and the ground station. The advantages are significant; VBR methods can increase the daily data rate of a ground station by a factor of 2.5 [8], and we will show that pattern synthesis can reduce the required number of antennas for a ground station by a factor of ten.

To the best of the authors' knowledge, no other papers have investigated the use of array pattern synthesis or variable bit rate methods to maximize the downlink capacity of an array for LEO satellite communications. Although the array described in [1] will have a dedicated subarray to increase the gain of the array near the horizon, this only mitigates the inefficiencies and it is not an analytically optimal solution.

The X-band downlink on the satellite EO-1 was chosen as the reference link for this analysis. This satellite is located at an altitude of 707 km and has a sun-synchronous orbit with an inclination of 98°. When this satellite is directly over a ground station, the required gain over noise temperature (G/T) for the ground station is 10.25 dB, accounting for required margins [2].

II. THE SPACE-FED LENS

A space-fed lens, which is fundamentally analogous to a Rotmann lens [3,4] except that it is planar, can form beams in the entire half-space and is light-weight and inexpensive. The lens is fabricated using standard printed circuit board technology [5-7]. It can be viewed as a hardware discrete Fourier transform of an arbitrary linear combination of plane waves incident on a focal surface. The wavefront is sampled at the incidence plane by an array of antenna elements; each sample is then appropriately time-delayed and re-radiated onto a focal surface by a second array of antennas. The fields on the focal surface are sampled so that each focal-plane antenna element (also called a detector) preferentially receives waves incident from a single direction. This is a discretized version of an optical dielectric lens which is thicker in the middle, i.e. has a larger delay in the middle [4]. Beamforming through a SFL at the front end has advantages in terms of reduced complexity, cost of digital hardware, and computational load, especially for large arrays.

A. Design of the SFL and its switching network

The presented SFL has only one degree of freedom: the delay line lengths [4]. It is implemented using standard planar circuit technology on a 0.381mm-thick Rogers TMM 6 substrate, and incorporates low-noise amplifiers (Hittite HMC462LP5) at the focal-surface antennas. This SFL provides polarization conversion from RHCP at the non-feed side to linear polarization at the feed side. Simulations of a RHCP truncated-corner patch element show 3.4dB of gain and 0.1dB of axial ratio, with S_{11}=-23 dB. The linearly-polarized square patches have 3.9dB of gain and S_{11}=-34dB.

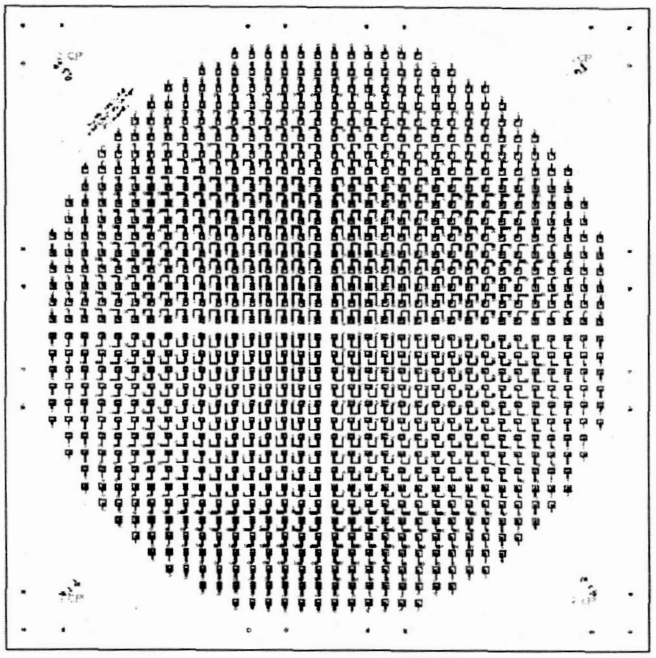

Fig. 1. Layout of the 952 antenna elements of both front-end array (red) and feed-side array (blue) that compose the SFL. Front-end antennas are RHCP because of the incoming signal, and feed-side antennas are linearly polarized for design simplicity and reducing inter-element coupling.

The true time delay is implemented with 50Ω microstrip lines. The element pairs are connected via interconnects with 0.5dB of insertion loss. The array, shown in Fig. 1, has 952 elements in a 0.75m diameter aperture. On both sides, elements are spaced at 0.6 wavelength to be near the Shannon-Nyquist sampling criterion. It produces a directivity D=36dB at 8.386GHz satisfying the system G/T requirements. Satellite tracking is performed by a switching network comprising thirty-two detectors on the focal surface. To increase the signal-to-noise ratio (SNR), each detector is directly linked to a low-noise amplifier (LNA). As shown, every other LNA is connected to the same bias voltage set and one of two 1:8 switches. This allows either discrete beam switching or continuous beamsteering by only modifying two sets of bias voltages. Fig. 2 shows a simplified version of this switching network with sixteen detectors, instead of thirty-two, to give a good understanding without loss of generality.

B. Simulation Results

The far field patterns of the thirty-two beams are given by Fig. 3. These beams uniformly cover the range of ±40 degrees off the local SFL zenith. In the worst case, the scalloping loss is 1.6dB. The envelope of these patterns determines the scan loss, which follows approximately the usual $\cos\theta$ law. This figure also shows that side lobe levels are very low in the scanning zone. The boresight levels will be reduced by

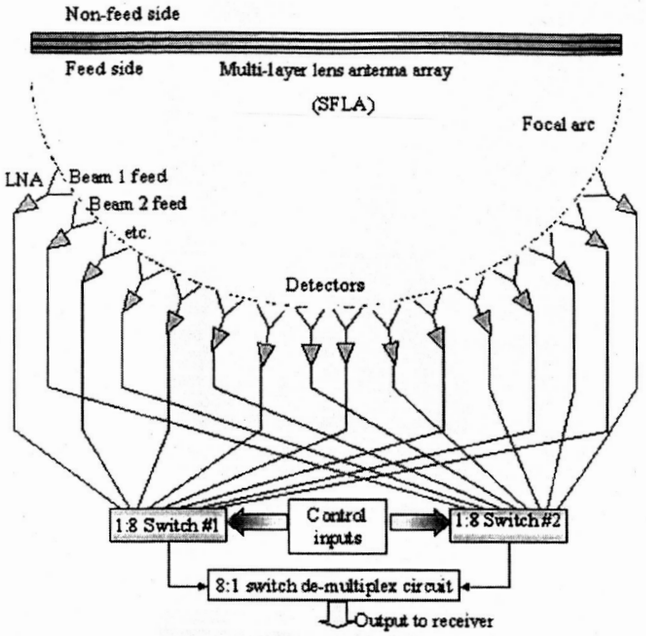

Fig. 2. A simplified version of the switching network with sixteen detectors. To increase the SNR, each detector is directly linked to an LNA. Every other LNA is connected to the same bias voltage set and one of two 1:8 switches. This allows either discrete beam switching or continuous beamsteering by only modifying two sets of bias voltages.

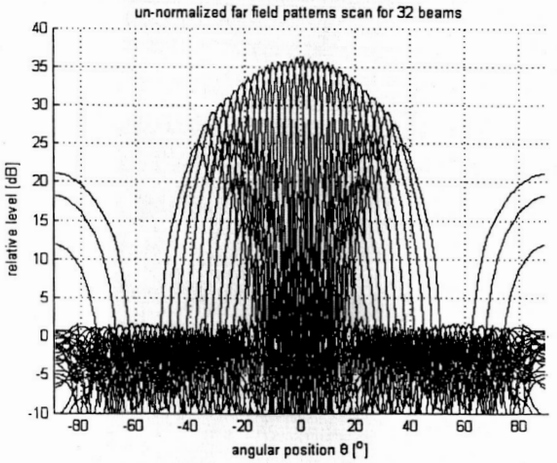

Fig. 3. Scan loss and un-normalized radiation pattern for 32 beams. Scalloping loss is better than 1.6dB (worst case).

placing absorbers in these directions. Fig. 4 emphasizes the degradation in the patterns when the considered beam is off the local Zenith, by showing the power distribution on the focal arc. At the Zenith (Fig. 4a) the beam is perfectly symmetric with side lobe levels lower than 30dB. At 20 degrees off the Zenith (Fig. 4b) there is no longer a focus point, but still a zone of good focus, and this creates higher side lobe levels.

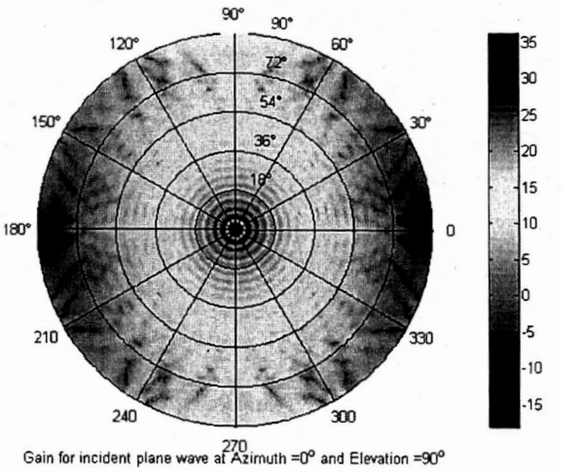

(a)

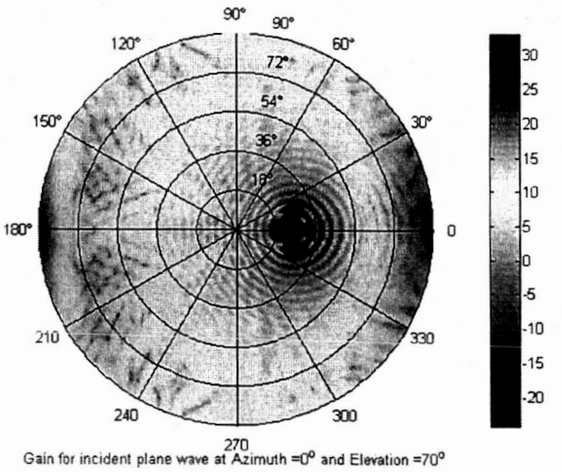

(b)

Fig. 4. Images on focal surfaces for incoming beams (a) at the Zenith and (b) at 70 degrees of elevation (20 degrees off the local Zenith).

These phenomena increase as the beam goes off the SFL local Zenith.

To cover 160 degrees with two SFLs in about 15 to 18 minutes, each beam has to be turned on for 15 seconds. This permits the use of a slow switching network.

III. FERROELECTRIC REFLECTARRAY ANTENNA

A scanning reflectarray consists of a flat surface with diameter D containing N integrated phase shifters and N patch radiators that is illuminated by a single feed at a virtual focus located a distance f from the surface such that $f/D \approx 1$. The modulated signal from the feed passes through the N reflect-mode phase shifters and is re-radiated as a focused beam in essentially any preferred direction in the hemisphere in front of the antenna, as in a conventional phased array. The control

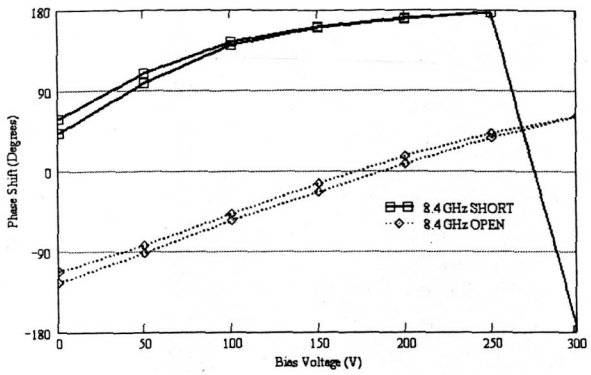

Fig. 5. Insertion phase of the hybrid (ferroelectric/semiconductor) X-band phase shifter with the termination in each state (open- or short-circuited).

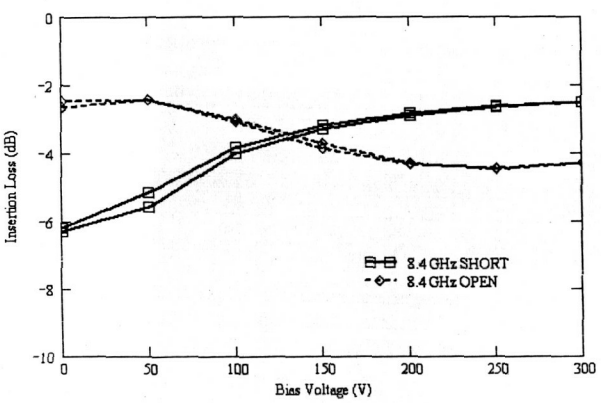

Fig. 6. Insertion loss envelope of the hybrid (ferroelectric/semiconductor) X-band phase shifter with the termination in each state (open- or short-circuited).

algorithm is nearly identical to that of a conventional phased array, the exception being an a priori setting of all phase shifters to compensate for the spherical wave-front from the feed. That is, the signal from the feed reaches the central element of the aperture before it reaches elements toward the perimeter. Of course, the physics, insofar as inter-element spacing, mutual coupling, scan loss, etc. is concerned, is the same as for a conventional directly radiating phased array.

One difficulty with implementing such an array arises from the fact that the phase shifters are necessarily between the feed horn and the patch radiating elements. Hence, they introduce line loss in front of the first stage low noise amplifier (LNA) and cause system noise temperature to escalate.

A hybrid X-band phase shifter consisting of four cascaded coupled microstrip lines patterned over 400 nm thick laser ablated $Ba_{0.50}Sr_{0.50}TiO_3$ films, followed by a silicon (Si) diode switch, has been designed, fabricated and tested. The ferroelectric section provides nominally 180 degrees of analog phase shift. Basically, as a bias from 0 to 350 V is applied across the coupled line electrodes, the relative dielectric constant of the film tunes from about 2000 to 800, thereby modifying the propagation constant. The ferroelectric films are, of course, excellent dielectrics and the current draw is negligible so there is virtually no power consumption. The beam lead Si diode switch is appended to the last coupled microstrip section and toggles between an open and virtual short circuit realized with a quarter-wave radial stub. This results in a "digital" transition between a reflection coefficient with magnitude near unity and phase of ≈ 0 degrees and ≈ 180 degrees, respectively. Thus, a full 2π phase shift is possible. The insertion phase of the phase shifter is shown in Fig. 5.

The insertion loss of the hybrid phase shifter is shown in Fig. 6. The hybrid phase shifter demonstrated an average loss of about 3.5 dB (over a 10 % bandwidth). The difference between the open- and short-circuited termination is very close to the predicted 180 degrees. The X-band reflectarray will be based on a 615 element, 19 GHz prototype. But instead of full two-dimensional electronic steering, the array will use one hybrid phase shifter per row to achieve elevation control electronically. But azimuth control will be done mechanically using a stepper motor and turnstile arrangement. This approach was selected to minimize cost. The 19 GHz prototype is shown in Fig. 7 for reference.

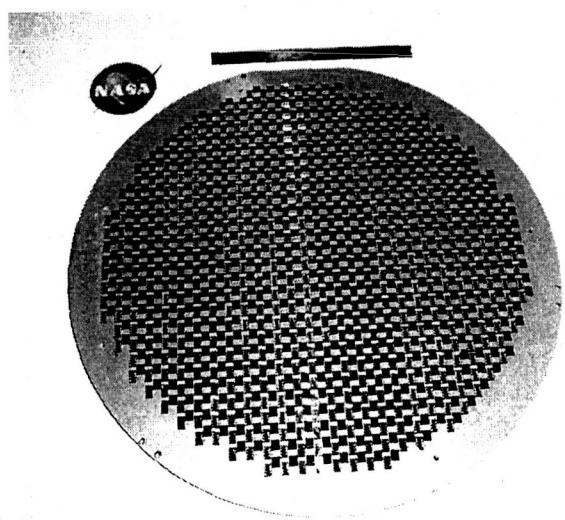

Fig. 7. 615 element, 19 GHz ferroelectric prototype array. The diameter is 28 cm.

IV. DOWNLOAD CAPACITY ANALYSIS

A. Introduction

To compare the various network configurations, we use a metric defined as the daily bit rate (DBR) of the ground station. The DBR represents the average number of bits that a

ground station can receive from the satellite in a 24-hour period.

A probabilistic approach is used to solve this problem. A probability density function is first derived to describe the likelihood that the subsatellite point is within an arbitrary region on the surface of the Earth. Next, an expression is created to describe the probability that the satellite is located in a region where a communications link can be established with the ground station. This expression is modified to include the effects of variable bit rates. The details of this analysis can be found in [8].

When EO-1 is near the horizon, the path loss on the link is 12dB higher than when the satellite is at zenith. Since the required gain of the array is determined by the path loss at the lowest desired elevation (LDE), an array of dish antennas will have more gain at higher elevation angles than is necessary for demodulation. If some type of pattern synthesis is used, then the ratio of the received energy per bit to the noise spectral height (E_B/N_0) will be independent of the elevation angle of the satellite. This will increase the DBR of the network without imposing the requirements of a variable bit rate method [8].

B. Pattern Synthesis

The type of pattern synthesis in this paper applies to electronically steered arrays with scanning loss or directional elements. The peak mainlobe gain in these arrays diminishes as the array is steered away from boresight [9]. Since several of these steered arrays are used in a ground station, the boresight directions can be different. In this type of pattern synthesis, the boresight directions of the phased arrays in the ground station are optimized so the adaptive combination of the phased array outputs yields the highest possible DBR.

This optimization will be applied to the SFLs, which will be mechanically steered in azimuth and electronically steered in elevation. Therefore, the SFLs will have scanning loss only as a function of elevation. Fig. 8(a) shows three SFLs, on azimuth turntables, sharing the same boresight direction and steered to the same target. In Fig. 8(b) each SFL has a different tilt, or boresight, direction but the mainlobes are steered to the same target location. Thus, for a given target location, each SFL exhibits a different value for scanning loss.

This scanning loss can be described by the function $G(\psi)$, where ψ is the elevation angle off-boresight, such that $G(0)=1$. If the peak power gain of the SFL in the boresight direction is given by a constant, A, then the power gain of the SFL when scanned to the angle ψ is $AG(\psi)$. The path loss between the ground station and the satellite can be defined as $L_P(\theta)$, where θ is the elevation angle of the satellite. If there are N SFLs and no other loss mechanisms, then the part of the link gain that depends only on the path loss and the SFL mainlobe gains can be expressed by

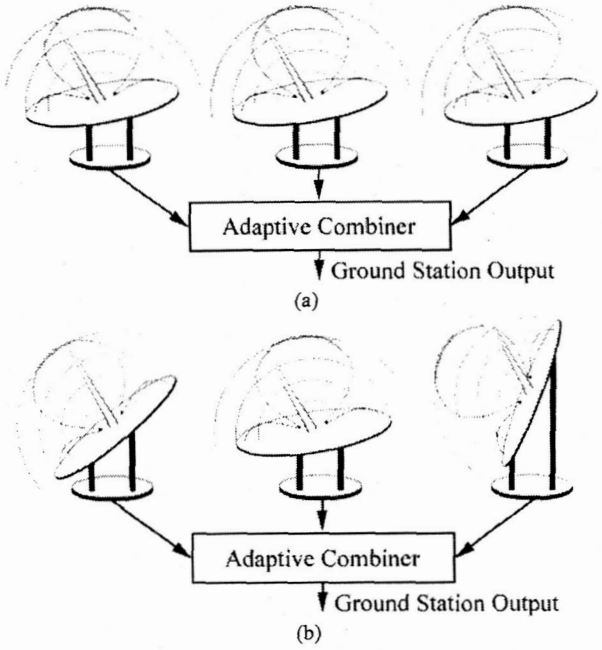

Fig. 8. Possible ground station configurations using the Space-fed Lens (SFL). The SFLs in (a) are all tilted to the same angle. The SFLs in (b) are tilted at different angles. The scan loss behavior is overlaid with 10dB intervals.

$$G_L(\theta)=\left[A\cdot\sum_{n=1}^{N}G(\theta-\psi_n)\right]\Big/L_p(\theta), \qquad (1)$$

where ψ_n is the boresight direction in elevation of the Nth Space-fed Lens. Genetic algorithms can optimize the values of ψ to make E_B/N_0 independent of the satellite's elevation.

Fig. 9 contains plots of $G_L(\theta)L_P(90°)$ for two cases. The optimized design has a LDE of 5° with eight antennas; despite the slightly lower gain and high scan loss of the SFL, this is only one more than the array of 0.75m dishes requires. The uniform array has a LDE of only 23° and an excess gain of more than 10dB at some angles. Approximately 80 antennas in the uniform array would be required to achieve an LDE of 5°, hence our claim in Section I of a factor of 10 reduction in the number of antennas. The DBR of the optimized array is almost four times that of the uniform array.

C. Simulation Results

The orbital descriptions used throughout this paper, in addition to the equations in [10], were used to develop a numerical network simulator. This generated network data for various configurations of ground stations at various locations. The simulator switched the transmission between ground sta-

tions by selecting the ground station with the highest E_B/N_0 for transmission at any given instant in time. The DBR was found by averaging the integrated capacity of many orbits and multiplying this capacity by the number of orbits per day.

The design goal for these networks was to meet or exceed the DBR of a single 11m dish antenna downlink station located at the Poker Flats facility in Alaska. For the purpose of this analysis the minimum LDE is restricted to 5° above the horizon. In all cases, the threshold signal strength for demodulation is taken as 6.5dB.

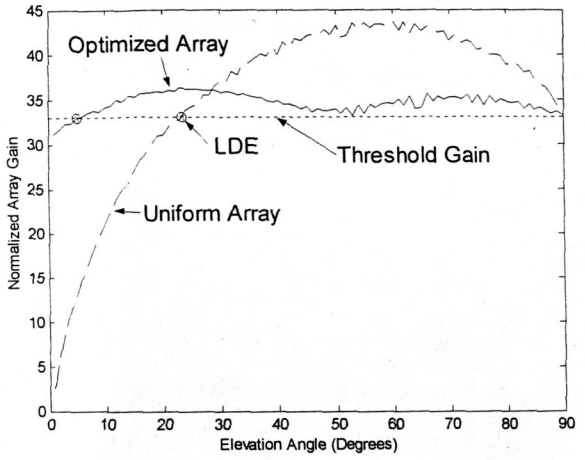

Fig. 9. The normalized link gains of the optimized SFL array and the uniform array as a function of elevation angle.

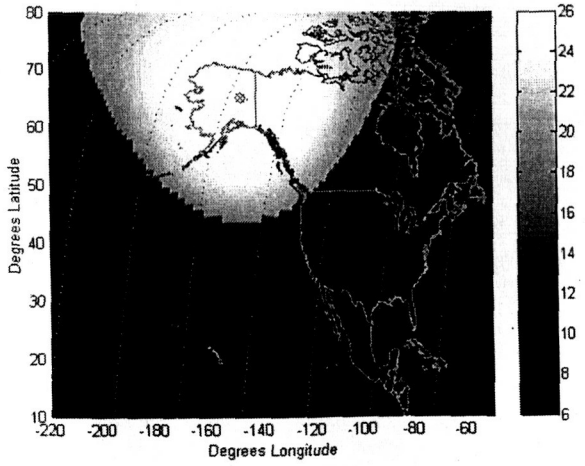

Fig. 10. Received signal strength as a function of the subsatellite point for a single downlink station located at the Poker Flats site.

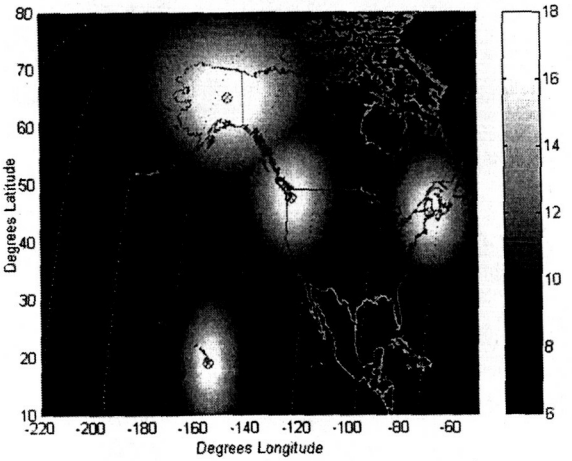

Fig. 11. Received signal strength as a function of the subsatellite point for four downlink stations, located in Hawaii, Washington, and Maine. The shading scale range is different than Fig. 5 to enhance readability.

Fig. 10 shows the received E_B/N_0 as a function of the position of the subsatellite point, for the reference case of a single 11m dish antenna at Poker Flats. The boundary of the coverage area for this antenna is defined by the LDE rather than the minimum signal strength. Fig. 11 shows the signal strength for a network of four downlink stations; each downlink station comprises several 0.75m dish antennas. The stations located in Hawaii, Washington, and Maine each use three antennas; the station in Alaska uses four.

Table I contains DBR results for a number of different network configurations. The variables in the network include the number of ground stations, the position of the ground stations, the number of antennas per ground station, and the data rate. Both fixed and variable data rate models are considered. All but the last assume 0.75m dish antennas. The last one uses SFLs with optimized boresight directions. We observe that several networks produce DBRs comparable to the Poker Flats facility; among these is the last 50 Mbps network, which corresponds to Fig. 11 and uses a total of only thirteen 0.75m dish antennas.

V. CONCLUSIONS

Using a simple path loss model, we have shown that there exist several possible small networks of ground nodes utilizing phased array antennas that can provide an average daily download capacity for the satellite EO-1 equaling or exceeding that of an 11m dish in Alaska. Two candidate phased array technologies have been reviewed. Optimization of the boresight directions of the phased arrays has been shown to effectively counter the degradation of the network capacity caused by scanning loss.

REFERENCES

[1] B. Tomasic, J. Turtle, S. Liu, R. Schmier, S. Bharj, and P. Oleski, "The geodesic dome phased array antenna for satellite control and communication – subarray design, development, and demonstration," presented at the 2003 IEEE Int. Symposium, Oct. 14-17, pp. 411-416.

[2] *Radio Frequency Interface Control Document (RFICD) Between the Earth Orbiter (EO)-1 Spacecraft and the Spaceflight Tracking and Data Network (STDN),* National Aeronautics and Space Administration, Goddard Space Flight Center, November 2000.

[3] W. Rotman, R.F. Turner, "Wide-angle microwave lens for line source applications," IEEE Trans. Antennas Propagat., AP-11, pp.623-632, 1963.

[4] D.T. McGrath, "Planar three-dimensional constrained lenses," IEEE Trans. on Antennas and Propagations, pp. 46-50, Jan. 1986.

[5] S. Romisch, N. Shino, D. Popovic, P. Bell, Z. Popovic, "Multibeam planar discrete millimeter-wave lens for fixed-formation satellites," in the Proc. of the 27th General Assembly of the International Union of Radio Science (URSI), Maastricht, Netherlands, Aug. 2002.

[6] R.Q. Lee, S. Romisch, Z. Popovic, "Multi-Beam Phased Array Antennas," 26th Annual Antenna Applications Symposium, Sept. 2002, Monticello, Illinois.

[7] D. Popovic, Z. Popovic, "Multibeam antennas with polarization and angle diversity," *IEEE Trans. Antennas and Propagat., Special Issue on Wireless Communications*, pp. 651-657, May 2002.

[8] W. C. Barott, M. A. Ingram, and P. G. Steffes, "A distributed network for high capacity downloads from LEO satellites," submitted to the IEEE Global Communications Conference (GLOBECOM 2005), St. Louis, MO., 28 Nov.-2 Dec, 2005.

[9] R. J. Mailloux, *Phased Array Antenna Handbook*, Boston: Artech House, 1993.

[10] T. Pratt and C. W. Bostian, *Satellite Communications,* New York: Wiley, 1986, pp. 11-30.

TABLE I
NETWORK CONFIGURATIONS AND PERFORMANCE

TX Rate (Mbps)	Network	Total Number of Antennas	Daily Bit Rate (GB)
105	11m (PF) -- Reference	1	585
50	7 x2 (S, B)	14	279
50	3 x2 (S, B)	6	270
50, 100	3 x2 (S, B)	6	395
50, 100, 200	3 x2 (S, B)	6	497
50, 100	3 x3 (S, B, T)	9	501
50, 100, 200	3 x3 (S, B, T)	9	642
105	3 x2 (S, B)	6	246
105	7 x2 (S, B)	14	587
105	5 x3 (C, H, DC)	15	545
105	5 x2 (H, DC) 6 x1 (C)	16	578
50	3 x4 (H, S, B, T)	12	427
50	3 x3 (S, B, H) 4 x1 (PF)	13	594
105	8 SFL x2 (S, B)	16	587

Network layout format is: Number of antennas per station x Number of stations (Station codes). Station codes include: Bangor, Maine (B), Stockton, California (C), Washington, D.C. (DC), Honolulu, Hawaii (H), Poker Flats, Alaska (PF), Seattle, Washington (S), and Corpus Christi, Texas (T).